Single- and Multiphoton Turn-On Fluorescent Fe^{3+} Sensors Based on Bis(rhodamine)

Aruna J. Weerasinghe, Carla Schmiesing, Shankar Varaganti, Guda Ramakrishna,* and Ekkehard Sinn*

Department of Chemistry, Western Michigan University, Kalamazoo Michigan 49008

Received: April 16, 2010; Revised Manuscript Received: June 14, 2010

Selective and sensitive turn-on fluorescent Fe^{3+} sensors based on novel bis(rhodamine) dye molecules are reported. The compounds are synthesized with very high yields and characterized with NMR, ESI mass spectrometry, and elemental analysis. Single- and two-photon fluorescence enhancement is observed for both molecules in the presence of Fe^{3+}. High selectivity and sensitivity is observed over other metal ions and is shown to be due mainly to the spirolactam ring-opening power of Fe^{3+}. All measurements are made in buffer environments simulating biological conditions to facilitate single- and multiphoton fluorescence imaging of Fe^{3+} in vivo and in vitro. Larger enhancement of fluorescence for both one- and two-photon excitation makes them suitable candidates for fluorescent labeling of biological systems. Two photon cross-section and time-resolved fluorescence measurements are utilized to understand the selectivity of the present sensors for Fe^{3+}-sensing.

1. Introduction

Detection of transition metals has become important due to their vital role in biological and environmental applications.[1−5] Detection of trace amounts of Fe^{3+} is of great importance as it is an important transition metal for all organisms and disorders in its metabolism cause anemia, liver and kidney damage, diabetes, and heart failure.[6,7] Very few sensors for Fe^{3+} have been reported despite its importance in many biochemical processes at the cellular level.[8−13] Furthermore, Fe^{3+} is a well-known fluorescence quencher due to its paramagnetic nature, which makes it difficult to develop a turn-on fluorescent sensor and more noteworthy to develop a sensitive one. Several methods have been reported for detecting iron including atomic absorption spectroscopy,[14] colorimetry,[15] spectrophotometry,[16−18] and voltammetry[19] techniques, which generally require sophisticated equipment, tedious sample preparation procedures, and trained operators. Therefore "naked eye" sensors have advantages over other methods in being easy to operate, portable, and not requiring sophisticated instrumentation. In the recent past, several attempts have been made to develop chemosensors to detect paramagnetic species.[20−26] Among different sensors, rhodamine-B derivatives and their ring-open reaction have received greater attention following the report of a rhodamine-B hydrazine sensor for Cu^{2+} by Czarnik et al.[27] Ring-closed rhodamine-B derivatives are colorless and nonfluorescent, whereas the ring-open forms are strongly fluorescent and pink in color.[28] Several successful attempts have been made to develop selective fluorescent sensors based on rhodamine B, for Cu^{2+},[29−31] Pb^{2+},[32] Hg^{2+},[33−41] and Cr^{3+}.[42] In all these sensors, the mechanism involves the formation of a ring-opened form of the spirolactam upon cation binding, resulting in fluorescence enhancement (550−600 nm). However, selectivity and sensitivity remain problems even with this approach. Thus, in the present investigation, novel bis(rhodamine) architecture is developed to increase the selectivity and sensitivity for detection.

Although fluorescence signals and their enhancement can be investigated with fluorescent molecular sensors, conventional fluorescence microscopy for imaging metal ions in biological systems with visible light is resolution limited due to image blurring by out-of-focus light. This limitation can be rectified with two photon laser scanning microscopy, which needs sensors to show enhanced two photon excited fluorescence.[43,44] Further, multiphoton or two photon excitation-based sensing can be used to detect analytes in a stand-off excitation and detection approach which will be utilized to probe complex biological and environmental conditions. Multiphoton excitation uses near-infrared light which has lower scattering and higher penetration depth even in cloudy and biological environments.[45] Recently, multiphoton excitation has been demonstrated for successful detection of nerve gases and energetic materials.[45,46] Two photon turn on sensors are also discovered for Zn^{2+} as well as some biological molecules.[47−49] In the present investigation, sensors are carefully engineered so that they are not only good sensors with one photon excitation but also excellent two photon turn on sensors. Our sensors are based on rhodamine derivatives as they possess large two photon cross sections for commercially available dye molecules. In this paper, we report two new bis(rhodamine)-based turn-on fluorescent sensors **1** and **2** (Scheme 1) for Fe^{3+}. Both show very high sensitivity and selectivity toward Fe^{3+} over other metal ions and are even higher with two photon excitation over conventional one photon excitation.

2. Experimental Section

2.1. Materials. Rhodamine B was purchased from Alfa Aesar. All the other chemicals were of reagent grade purchased from Sigma Aldrich and used without further purification. Nanopure water was used for making buffer solutions.

***Synthesis of* 1.** A solution of **3**[29] (0.74 g, 1.62 mmol) and pyridine-2,6-dicarboxaldehyde (0.1 g, 0.74 mmol) in 20 mL of ethanol was refluxed for 12 h. The mixture was allowed to cool to room temperature. The solid formed was filtered and air-dried (0.64 g, 85.4%). Mp = 266−268 °C. ^{1}H NMR (400 MHz, $CDCl_3$): δ 1.12 (24H, t, J = 6.9 Hz), 3.29 (16H, q, J = 6.9

* To whom correspondence should be addressed. E-mail: (E.S.) ekk.sinn@wmich.edu; (G.R.) rama.guda@wmich.edu.

10.1021/jp1034568
Published on Web 07/06/2010

SCHEME 1: Synthetic Pathway of 1 and 2

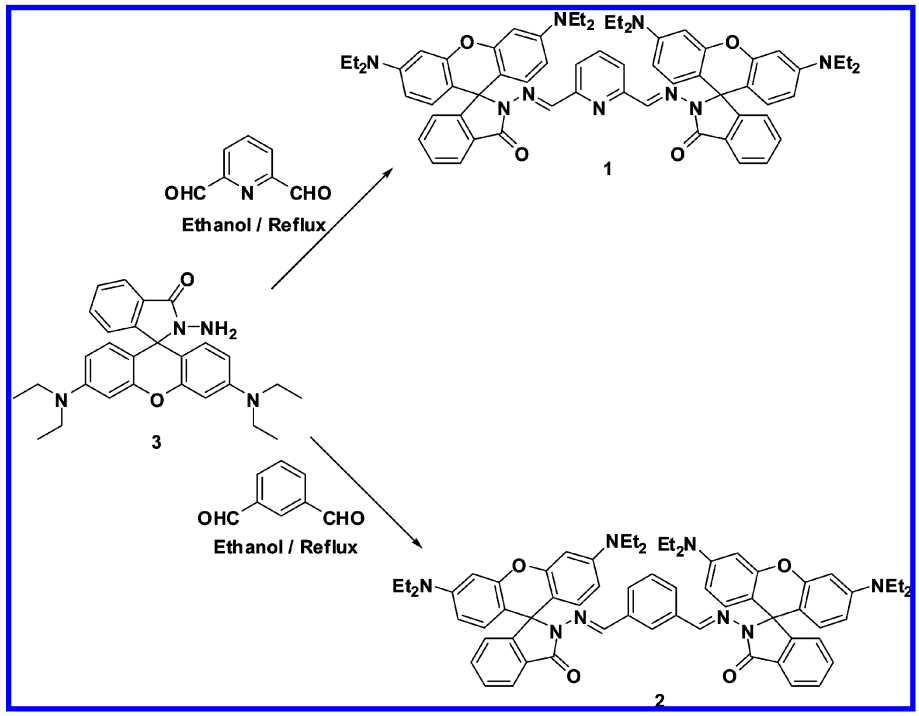

Hz), 6.19 (4H, dd, $J = 8.8$ Hz, 2.6 Hz), 6.43 (4H, d, $J = 2.6$ Hz), 6.47 (4H, d, $J = 8.8$ Hz), 7.11 (2H, d, $J = 7.3$ Hz), 7.46 (5H, m), 7.71 (2H, d, $J = 7.7$ Hz), 7.96 (2H, d, $J = 6.6$ Hz), 8.71 (2H, s). ^{13}C NMR (100 MHz, $CDCl_3$): δ 12.74, 44.39, 66.30, 98.20, 106.07, 107.94, 120.41, 123.56, 123.98, 127.80, 128.32, 129.16, 133.56, 135.94, 148.18, 148.97, 151.89, 153.29, 154.15, 165.09. ESI-MS. 1034.67 [M + Na]. Analysis calcd: C, 74.75; H, 6.47; N, 12.45. Found: C, 74.83; H, 6.86; N, 12.65.

***Synthesis of* 2.** A solution of **3**[29] (1.0 g, 2.2 mmol) and isophthalaldehyde (0.13 g, 0.97 mmol) in 20 mL of ethanol was refluxed for 12 h. The mixture was allowed to cool to room temperature. The solid was filtered and air-dried (0.78 g, 79.6%). Mp = 244−246 °C. ^{1}H NMR (400 MHz, $CDCl_3$): δ 1.13 (24H, t, $J = 6.9$ Hz), 3.29 (16H, q, $J = 6.9$ Hz), 6.18 (4H, d, $J = 8.8$ Hz), 6.42 (4H, s), 6.49 (4H, d, $J = 8.8$ Hz), 7.08 (2H, d, $J = 7.3$ Hz), 7.17 (1H, t, $J = 7.7$ Hz), 7.43 (5H, m), 7.56 (2H, d, $J = 7.7$ Hz), 7.97 (2H, d, $J = 6.9$ Hz), 8.33 (2H, s). ^{13}C NMR (100 MHz, $CDCl_3$): δ 12.73, 44.39, 65.87, 98.19, 105.75, 108.03, 123.49, 123.74, 127.70, 127.90, 128.13, 128.23, 128.30, 128.59, 133.49, 135.45, 146.13, 149.04, 152.39, 152.93, 165.26. ESI-MS. 1011.58 [M + 1]. Analysis calcd: C, 76.01; H, 6.58; N, 11.08. Found: C, 75.67; H, 6.85; N, 11.19.

2.2. Methods. Optical absorption measurements were carried out using a Shimadzu UV 2101 PC absorption spectrometer at room temperature. Fluorescence measurements were carried out using an Edinburgh FS920 spectrofluorimeter. Stock solutions of metal ions (5×10^{-3} M) were prepared using nitrates [$Cr(NO_3)_3$, $Zn(NO_3)_2$, $Ni(NO_3)_2$, $Pb(NO_3)_2$, $Cd(NO_3)_2$, $Hg(NO_3)_2$, $NaNO_3$, KNO_3] or chlorides [$MnCl_2$, $CuCl_2$, $FeCl_3$, $FeCl_2$, $CaCl_2$]. All the solutions were prepared in water. The stock solutions of compounds **1** and **2** (0.2 mM) were prepared in 75% CH_3CN, 25% 0.01 M Tris-HCl buffer. Fluorescence and UV absorption studies were performed using a 5 μM solution of **1** and **2** in 75% CH_3CN, 25% 0.01 M Tris-HCl buffer with appropriate amounts of metal ions. Solutions were shaken for 1 min and allowed to stand for another 2 min before measuring the absorption and fluorescence. The excitation was performed at 510 nm for all the emission studies. Both excitation and emission slit widths were kept at 2 nm. All the ^{1}H NMR (400 MHz) and ^{13}C NMR (100 MHz) spectra were obtained on a JEOL eclipse instrument in chloroform-d_6.

Two photon sensing and the two-photon absorption cross sections (δ) measurements were carried out using the two-photon excited fluorescence (TPEF) method described elsewhere.[50] A 10^{-4} M Rhodamine 6G solution in methanol was used as the reference over a wavelength range of 720−900 nm with the cross sections of the standard reported earlier.[51] A broad-band Ti:Sapphire oscillator (Tsunami, Spectra Physics) was utilized for the investigations. A neutral density filter was used to change the power to measure the power dependence. Fluorescence from sensors-metal ions gave a slope of 2 indicating that it is indeed a two-photon absorption event.

Time-resolved fluorescence measurements of sensors **1** and **2** in the presence of metal ions were studied using the newly developed femtosecond fluorescence upconversion spectroscopy technique reported elsewhere.[50] The upconversion system used in our experiments was obtained from CDP systems and the design is similar to what has been published earlier.[52] Specifically, the system used frequency-doubled (400 nm) light from a mode-locked broad band Ti-sapphire laser (Spectra Physics, Tsunami, 800 nm). Polarization of the excitation beam for the anisotropy measurements was controlled using a Berek compensator and the sample was continuously rotated with a rotating cell 1 mm thickness. Horizontally polarized fluorescence emitted from the sample was up-converted in a nonlinear crystal of β-barium borate using a pump beam at 800 nm, which first passed through a variable delay line. Instrument response function (IRF) was measured using Raman scattering from water. Fitting the Gaussian peak from the Raman scattering yielded a sigma value of ~130 fs, which gives a full width half-maximum of ~250 fs. Spectral resolution was achieved by using a double monochromator and photomultiplier tube. The excitation average power varied but was around 4 ± 0.2 mW. Little degradation of the samples was observed during the measurements.

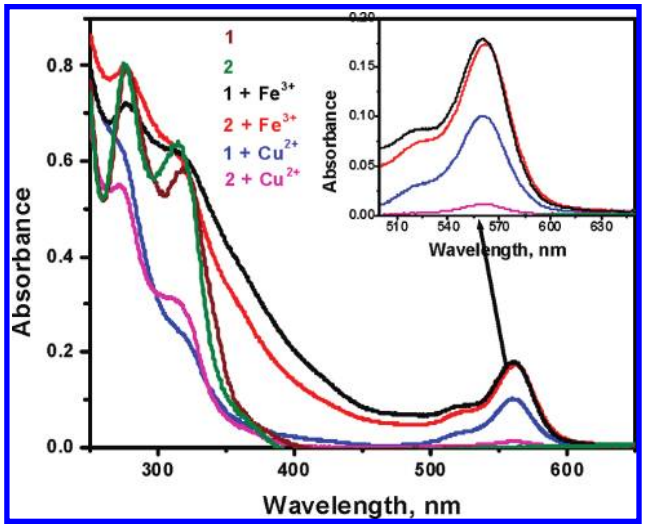

Figure 1. UV−vis absorption spectra of **1** and **2** (5 μM) with Fe^{3+} and Cu^{2+} (200 μM). Inset shows the enlarged spectra from 500 to 650 nm.

3. Results and Discussion

As shown in Scheme 1, compounds **1** and **2** were synthesized in high yield by refluxing **3**[29] with pyridine-2,6-dicarboxaldehyde and isophthalaldehyde in ethanol respectively. Their structures have been confirmed using ^{1}H NMR, ^{13}C NMR, ESI mass spectrometry, and elemental analysis (see Supporting Information). All the spectroscopic studies were performed in 75% CH_3CN, 25% 0.01 M Tris-HCl buffer system (pH = 7.00). Both compounds **1** and **2** were colorless and found to be very stable in the above-mentioned solution system for more than one week. Furthermore, the stabilities of the two compounds were tested over a wide range of pH and an increasing color change was observed with increasing acidity, indicating the formation of the ring-opened form (Supporting Information). Interestingly, compound **1** showed more sensitivity to pH than **2**, showing a greater color change below pH < 6. The absorption spectra of compounds **1** and **2** in buffer solutions did not show any peaks above 400 nm indicating the ring-closed spirolactone is predominant. In addition, a very weak fluorescence signal was observed at 580 nm upon excitation at 510 nm, confirming the presence of ring-closed spirolactone. The presence of the ring-closed form is further confirmed by the characteristic carbon resonances at δ 66.30 and 65.87 for **1** and **2** respectively. Thus, all the sensing and optical measurements for **1** and **2** were performed in buffer solution with a pH of 7 to keep the dye molecules in their ring closed form.

3.1. Steady-State Optical Properties. Figure 1 shows the absorption spectra of **1** and **2** (5 μM) in solution and in the presence of Cu^{2+} and Fe^{3+}. There is no absorption observed above 500 nm in the absence of metal ions indicating that only the ring-closed form is present. Addition of Fe^{3+} (200 μM) for both sensor molecules resulted in the appearance of the characteristic rhodamine B absorption at 560 nm with a shoulder at 520 nm due to the formation of the ring-opened spirolactam forms. Interestingly, Cu^{2+} also yielded a significant absorption enhancement with **1** but a much lower enhancement with **2** (Figure 1). However, the absorption increase at the same concentrations (200 μM) is lower than with Fe^{3+}. The results can be attributed to the differences in the association constants for **1** and **2** with Fe^{3+} and Cu^{2+}.

The addition of 200 μM (40 equivalents) of Fe^{3+} immediately yielded a pink solution with a strong fluorescence signal at 580 nm. There was 33-fold fluorescent enhancement for sensor **1** with Fe^{3+} (Figure 2) while sensor **2** yielded a 48-fold enhancement (Figure 3). The plot of measured fluorescence ($I_0/I-I_0$) against 1/[Fe^{3+}] showed a linear relationship (Supporting Information) confirming the formation of a 1:1 complex between **2** and Fe^{3+}. Sensor **1** also showed similar behavior for concentrations of Fe^{3+} in the range 150−237.5 μM. The binding constants, calculated using the Benesi-Hildebrand[53] method, were found to be 7.5×10^3 and 5.1×10^3 M^{-1} for **1** and **2** respectively. On the other hand, addition of Na^+, K^+, Ca^{2+}, Mn^{2+}, Fe^{2+}, Ni^{2+}, Zn^{2+}, Cd^{2+}, Hg^{2+}, or Pb^{2+} did not yield any color change (insets of Figure 2 and Figure 3). Sensor **1** showed slight fluorescent enhancement (3 times) with Cr^{3+} while other metals used in the experiment did not show any fluorescent enhancement. Similarly, sensor **2** also showed a slight emission enhancement (>5 times) with Cr^{3+} while the other metals showed no interference at all. Interestingly, Cu^{2+} did produce a small color change, though the spectroscopy and interaction of sensor **1** and **2** with Cu^{2+} are completely different from those **1** and **2** with of Fe^{3+}. The fluorescence enhancement observed

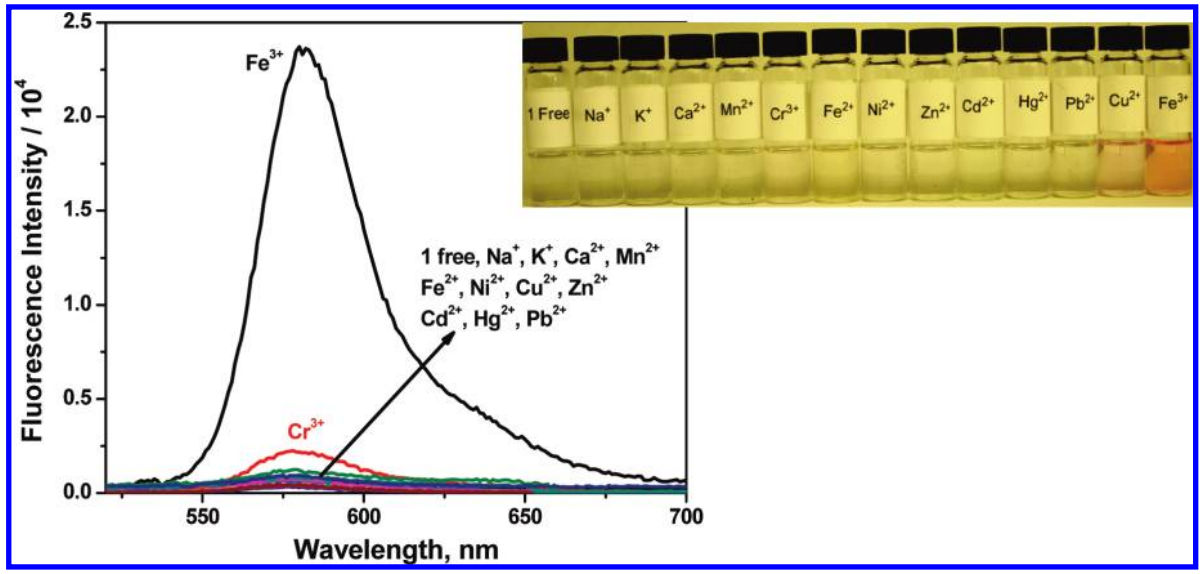

Figure 2. Fluorescence spectra of **1** (5 μM) in 75% CH_3CN, 25% 0.01 M Tris HCl buffer with different metal ions (200 μM). Insert shows the photo of sensor **1** with different metal ions (200 μM).

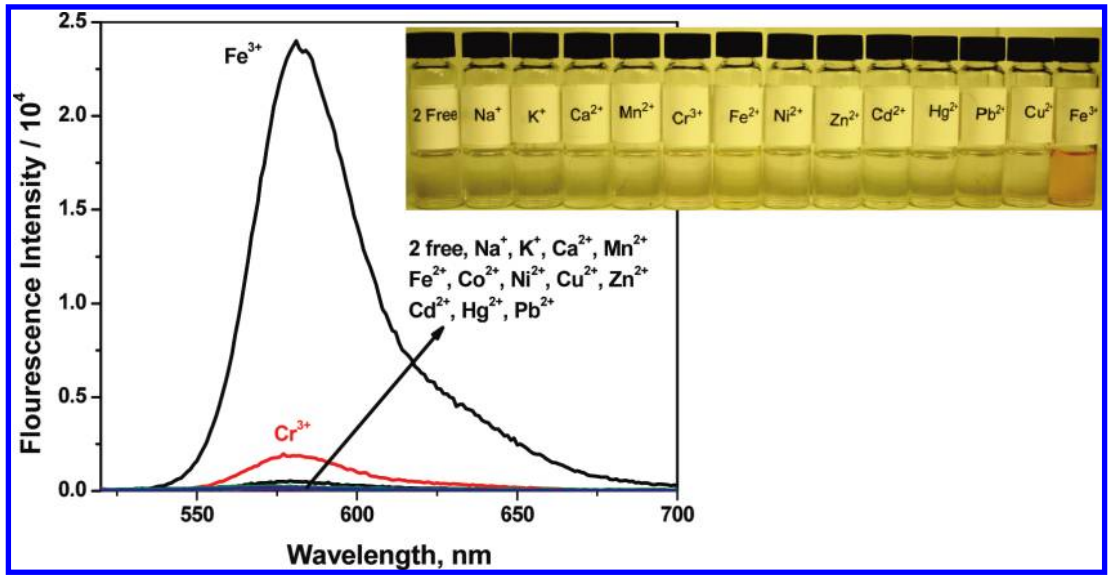

Figure 3. Fluorescence spectra of **2** (5 μM) in 75% CH_3CN, 25% 0.01 M Tris HCl buffer with different metal ions (200 μM). Insert shows the photo of sensor **2** with different metal ions (200 μM).

with Cu^{2+} was very small even though this ion was successful in opening the ring, as evident from the absorption spectrum (Figure 1). Other metal ions tested during the experiment did not show any absorption enhancement and consequently no fluorescence enhancement is expected or observed. These results show the excellent selectivity of sensors toward Fe^{3+} over other metal ions, which is further discussed below.

Fluorescence quantum yield measurements were carried out for the sensors **1** and **2** with Fe^{3+} and Cu^{2+} metal ions to understand the differences in fluorescence behavior observed, and the results show interesting trends. The fluorescence quantum yields for **1** with Fe^{3+} and Cu^{2+} are around 0.024 and 0.007, respectively, while the fluorescence quantum yields for **2** with Fe^{3+} and Cu^{2+} are around 0.048 and 0.018, respectively. It is observed that the fluorescence quantum yield is significantly lower for the sensors with both Fe^{3+} and Cu^{2+} when compared to free rhodamine B, which has a quantum yield close to unity. This might be due to the inherent quenching of fluorescence with inter-rhodamine interactions. However, the fluorescence quantum yield is very low for the sensors **1** and **2** in the presence of Cu^{2+} when compared to Fe^{3+}, and this is a possible reason for lower enhancement of fluorescence for sensors with Cu^{2+}. Further time-resolved fluorescence measurements with femtosecond fluorescence upconversion were carried out to resolve the conjecture.

3.2. Fluorescence Sensing: Single and Two Photon Excitation. As discussed above, the investigated sensors **1** and **2** show very good selectivity with turn-on fluorescence upon one-photon excitation. Two-photon fluorescence sensing measurements have been carried out for Fe^{3+} and Cu^{2+} with sensors **1** and **2** to reveal the differences between them. All the two-photon sensing measurements were carried out with excitation at 800 nm. Comparative enhancements observed for one-and two-photon excitations are shown in Figures 4 and 5, which indicate that the fluorescence enhancement has increased further with two- photon excitation than with one-photon excitation for both sensors in the presence of Fe^{3+}. However, the enhancement is minimal for Cu^{2+} in both excitations. The larger enhancements observed with two-photon excitation can be attributed to two factors. First, there is absorption interference from Fe^{3+} in the visible region, which influences the one-photon enhancement, while the two-photon enhancement is not influenced by such

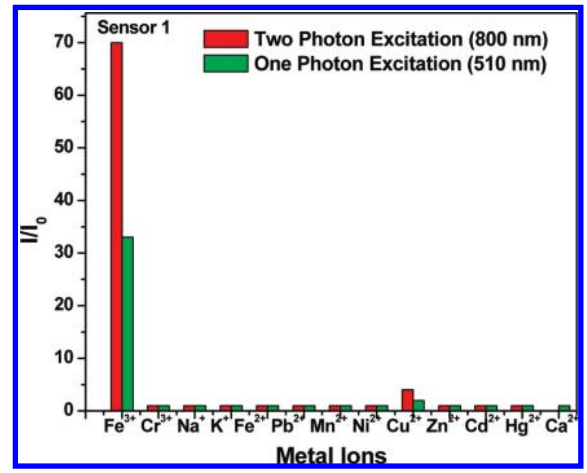

Figure 4. Fluorescence histogram plot of **1** (5 μM) at 585 nm upon addition of different metal ions (200 μM) in 75% CH_3CN, 25% 0.01 M Tris HCl buffer.

interference. Second, the presence of Fe^{3+} increases the two-photon cross-section since the metal ions open up the ring and increase the inter-rhodamine interaction. This in turn enhances the two-photon cross sections. Two-photon cross-section measurements have shown such inter-rhodamine interaction in the presence of metal ions (Supporting Information) and cross-section enhancement. Interestingly, the two-photon cross-section is larger for sensor **2** with Fe^{3+} than that of sensor **1** since pyridine bridging is influencing the conjugation between rhodamine units in a negative way. The present results show that these new sensors can be efficiently utilized for multiphoton imaging of Fe^{3+} in biological systems and complex environments because of their excellent two-photon excited fluorescence upon complexation. The histograms in Figure 4 and 5 clearly show that the sensors are highly selective for Fe^{3+} ion over all other metal ions. It is interesting to note that it is very easy to differentiate Fe^{2+} from Fe^{3+} with these sensors. The selectivity observed here is ascribed to the ability of Fe^{3+} to form a complex that can open the spirolactone ring. Other metal ions do not have the size advantage or the relative bonding strength to open up the spirolactone ring.

Sensitivity Measurements. Concentration dependent fluorescence measurements were carried out to monitor the sensitivity

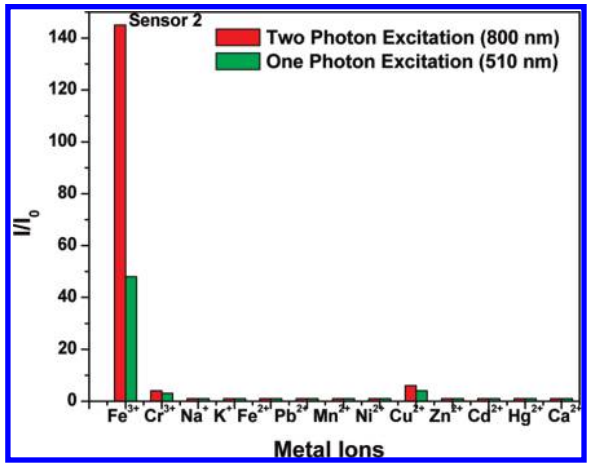

Figure 5. Fluorescence intensity of **2** (5 μM) at 585 nm upon addition of metal ions (200 μM) in 75% CH_3CN, 25% 0.01 M Tris HCl buffer.

for Fe^{3+} ion. Shown in Figure 6A,B are the concentration dependent fluorescence measurements monitored after excitation at 510 nm. Association constants calculated from such measurements are higher for sensors **1** and **2** with Fe^{3+} over other metal ions. It is observed that the sensitivities of **1** and **2** for Fe^{3+} are around 50 and 70 μM, respectively. Sensitivity is calculated by determining the concentration where the enhancement of fluorescence is three times that of the background. Similar sensitivity as that of one-photon excitation is observed for the two-photon excitation measurements. The present sensors are highly selective for Fe^{3+}, even differentiating it from Fe^{2+} with sensitivity in the micromolar region. Efforts are underway to improve the sensitivity to nanomolar concentration by appropriately designing the molecular sensors.

3.3. Fluorescence Upconversion Measurements. In an effort to understand the selectivity of the sensors **1** and **2** for Fe^{3+} over the other metal ions especially that of Cu^{2+} and the differences in fluorescence quantum yields, time-resolved fluorescence measurements were carried out. Time-resolved fluorescence measurements on the sensors **1** and **2** in presence of Cu^{2+} and Fe^{3+} were carried out with femtosecond fluorescence upconversion spectroscopy after excitation at 400 nm and monitoring the fluorescence at 580 nm (Figure 7). Fluorescence lifetime studies of sensor **1** with Cu^{2+} (Figure 7A) demonstrated the decay that was fitted with a multiexponential function with lifetimes of 220 fs (65.5%), 1.2 ps (32.2%), and >20 ps (2.3%), where the average lifetime is around 540 fs, indicating a faster intersystem crossing rate. By comparison with Fe^{3+} (Figure 7A), sensor **1** showed double exponential decay of 290 fs (88.9%) and 350 ps (11.1%). The average lifetime of **1** with Cu^{2+} is far shorter than that of **1** with Fe^{3+}, suggesting that the faster intersystem crossing caused by Cu^{2+} is the reason for observing little steady state fluorescence as well as lower fluorescence quantum yield. Interestingly, sensor **2** showed completely different behavior than did sensor **1** with both Cu^{2+} and Fe^{3+}. Two major decay components (3.4 ps (80%) and >20 ps (20%)) were observed for **1** with Cu^{2+}, while with Fe^{3+} it also yielded two lifetimes (3.7 ps (15.3%) and 330 ps (84.7%). Interestingly, the shorter lifetime component comprised 80% of the decay

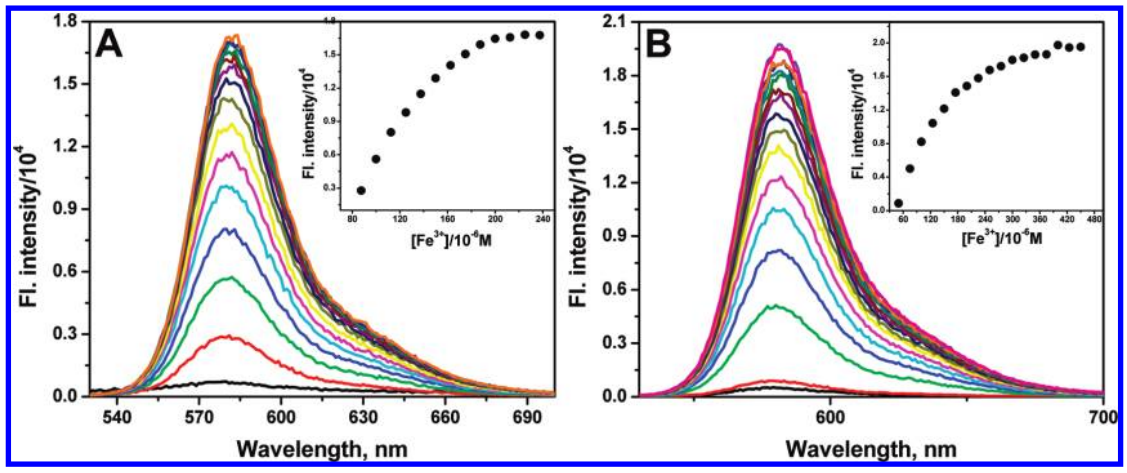

Figure 6. (A) Fluorescence titration of **1** (5 μM) in 75% CH_3CN, 25% 0.01 M Tris HCl buffer with Fe^{3+} and (B) fluorescent titration of **2** (5 μM) in 75% CH_3CN, 25% 0.01 M Tris HCl buffer with Fe^{3+}ions.

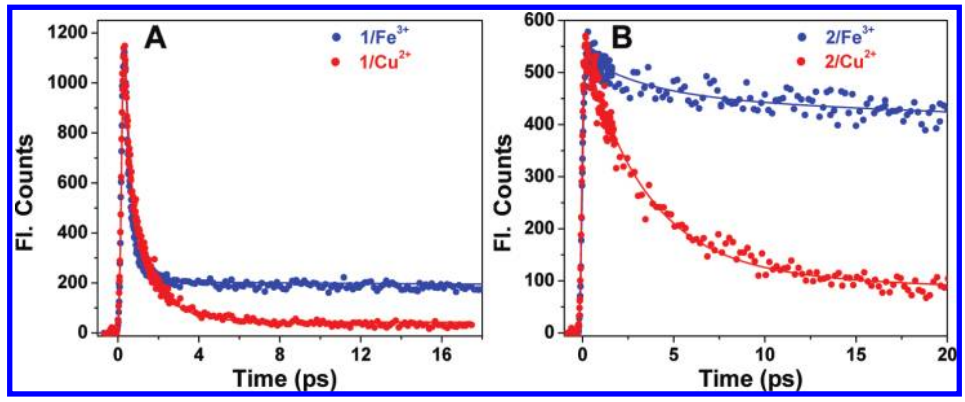

Figure 7. Fluorescence decay traces for sensors **1** and **2** in presence of Fe^{3+} and Cu^{2+}, respectively. The faster fluorescence decays with Cu^{2+} indicate ultrafast deactivation pathways.

SCHEME 2: Turn-on Fluorescence of Compound 1 in the Presence of Fe^{3+} with the Opening of the Two Spirolactam Rings[a]

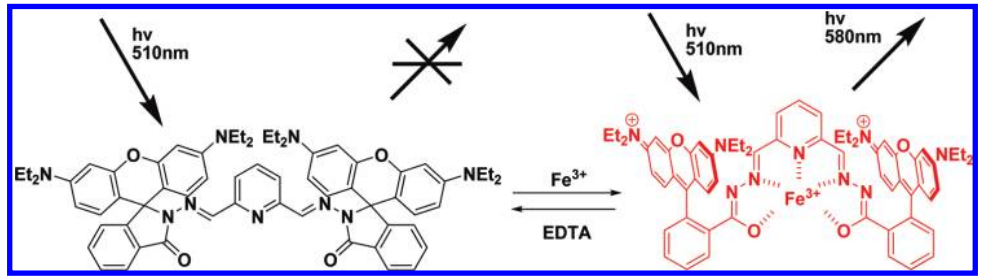

[a] Addition of EDTA reverses the sample to turn-off position.

while the longer lifetime component comprised only 20%. Here again, differences in the average lifetimes for **2** with Fe^{3+} and Cu^{2+} can explain the shift to lower values of the fluorescence quantum yield. It has to be noted here that the free rhodamine does not give any shorter components in its decay. The observed shorter lifetime components for sensors **1** and **2** point to the presence of nonradiative decay pathways that can be ascribed to inter-rhodamine interactions thus explaining the observed differences in fluorescence quantum yield of the sensors and rhodamine B.

Mechanism of Fluorescence Sensing. As discussed above, both sensors showed excellent selectivity toward Fe^{3+}. The color formation for both sensors with Fe^{3+} is ascribed to the ring-opening mechanism shown in Scheme 2. It is reasonable to suggest that the Fe^{3+} can bind with the amide oxygen that causes the ring-opening. The pyridine nitrogen does not make much contribution for Fe^{3+} binding, as indicated by the absence of a significant difference in emission enhancement for **1** and **2** with Fe^{3+}. Interestingly, there is a remarkable difference in Cu^{2+} binding with the sensors since **2** showed very small absorption enhancement compared to **1**. This suggests that the pyridine nitrogen plays a key role in Cu^{2+} binding. Furthermore, binding of Cu^{2+} and Fe^{3+} with **1** and **2** is reversible; the color disappears upon the addition of excess EDTA. The novel bis(rhodamine) architecture in the present investigation gives a selective sensor for Fe^{3+} based on ring open and ring closed forms of rhodamine B. These sensors also offer early passive detection of corrosion that may signal potential weakening of structural materials containing iron and steel. On the basis of the spectra in Figure 1, the two compounds used in conjunction offer a unique high-sensitivity sensor for Fe^{3+} even in the presence of large amounts of Cu^{2+}; fluorescence quantum yields further distinguish Fe^{3+} and eliminate false positives from Cu^{2+}.

4. Conclusions

Bis(rhodamine) derivatives with pyridine (**1**) and benzene (**2**) bridging groups are synthesized, which are highly selective and sensitive turn-on fluorescent sensors for Fe^{3+} ion. Enhancements in both one and two photon excited fluorescence is observed for both sensors with Fe^{3+} and suggests their application in biological imaging of Fe^{3+}-containing systems. Two photon fluorescence enhancement is greater than that of one photon excitation, which is ascribed to the greater two photon cross sections upon complexation and lower interference from metal ion absorption. Mechanistically, bis(rhodamine) derivatives have greater association constants with Fe^{3+} as they complex with the amide oxygen, thereby assisting the ring-opening of spirolactam, which gives rise to the luminescence. Since **1** and **2** behave similarly toward Fe^{3+}, it appears that the bridging pyridine is not of great importance in the complexation. On the other hand, Cu^{2+} was able to open the ring, which is evident from optical absorption; the fluorescence enhancement is significantly smaller than that of Fe^{3+}. Lower fluorescence quantum yields and ultrafast fluorescence deactivation pathways with Cu^{2+} are the reasons behind lower fluorescence enhancement when compared to Fe^{3+}. The present novel architecture of bis(rhodamine) can be further explored to obtain highly selective and sensitive sensors.

Acknowledgment. The authors wish to acknowledge the financial support under U.S. Army Grant W911QY-07-1-0003. The authors also would like thank Dr. Andre Venter for the help given to obtain ESI mass spectra. G.R. acknowledge the support of the Western Michigan University Faculty Research and Creative Activities Support Fund (FRACASF).

Supporting Information Available: Two photon cross-section measurements, NMR spectra, and additional spectra. This material is available free of charge via the Internet at http://pubs.acs.org.

References and Notes

(1) de Silva, A. P.; Gunaratne, H. Q. N.; Gunnlaugsson, T.; Huxley, A. J. M.; McCoy, C. P.; Radamacher, J. T.; Rice, T. E. *Chem. Rev.* **1997**, *97*, 1515.
(2) *Chemosensors for Ion and Molecule Recognition*; Czarnik, A. W., Desvergne, J.-P., Eds.; Kluwer: Dordrecht, The Netherlands, 1997.
(3) Valeur, B.; Leray, I. *Coord. Chem. Rev.* **2000**, *205*, 3. .
(4) Lin, W.; Long, L.; Yuan, L.; Cao, Z.; Feng, J. *Anal. Chim. Acta* **2009**, *634*, 262.
(5) Zhang, M.; Gao, Y.; Li, M.; Yu, M.; Li, F.; Li, L.; Zhu, M.; Zhang, J.; Yi, T.; Huang, C. *Tetrahedron Lett.* **2007**, *48*, 3709.
(6) Brugnara, C. *Clin. Chem.* **2003**, *49*, 1573.
(7) Zhang, X.-B.; Cheng, G.; Zhang, W.-J.; Shen, G.; Yu, R.-Q. *Talanta* **2007**, *71*, 171.
(8) Xiang, Y.; Tong, A. *Org. Lett.* **2006**, *8*, 1549.
(9) Tumambac, G. E.; Rosencrance, C. M.; Wolf, C. *Tetrahedron* **2004**, *60*, 11293.
(10) Liu, J.-M.; Zheng, Q.-Y.; Yang, J.-L.; Chen, C.-F.; Huang, Z.-T. *Tetrahedron Lett.* **2002**, *43*, 9209.
(11) Bricks, J. L.; Kovalchuk, A.; Trieflinger, C.; Nofz, M.; Buschel, M.; Tolmachev, A. I.; Daub, J.; Rurack, K. *J. Am. Chem. Soc.* **2005**, *127*, 13522.
(12) Mitra, A.; Ramanujam, B.; Rao, C. P. *Tetrahedron Lett.* **2009**, *50*, 776.
(13) Ghosh, S.; Chakrabarty, R.; Mukherjee, P. S. *Inorg. Chem.* **2009**, *48*, 549.
(14) Ohashi, A.; Ito, H.; Kanai, C.; Imura, H.; Ohashi, K. *Talanta.* **2005**, *65*, 525.
(15) Liang, Z.-Q.; Wang, C.-X.; Yang, J.-X.; Gao, H.-W.; Tiang, Y.-P.; Tao, X.-T.; Jiang, M.-H. *New. J. Chem.* **2007**, *31*, 906.
(16) Lunvongsa, S.; Oshima, M.; Motomizu, S. *Talanta* **2006**, *68*, 969.
(17) Tesfaldet, Z. O.; van Staden, J. F.; Stefan, R. I. *Talanta* **2004**, *64*, 1189.
(18) Gomes, D. M. C.; Segundo, M. A.; Lima, J. L. F. C.; Rangel, A. O. S. S. *Talanta* **2005**, *66*, 703.
(19) Bobrowski, A.; Nowak, K.; Zarebski, J. *Anal. Bioanal. Chem.* **2005**, *382*, 1691.

(20) Ghosh, P.; Bharadwaj, P. K.; Mandal, S.; Ghosh, S. *J. Am. Chem. Soc.* **1996**, *118*, 1553.
(21) Royzen, M.; Dai, Z.; Canary, W. J. *J. Am. Chem. Soc.* **2005**, *127*, 1612.
(22) Rurack, K.; Kollmannsberger, M.; Resch-Genger, U.; Daub, J. *J. Am. Chem. Soc.* **2000**, *122*, 968.
(23) Banthia, S.; Samanta, A. *J. Phys. Chem. B* **2006**, *110*, 6437.
(24) Prodi, L.; Bolletta, F.; Montalti, M.; Zaccheroni, N. *Coord. Chem. Rev.* **2000**, *205*, 59.
(25) Sankaran, N. B.; Banthia, S.; Das, A.; Samanta, A. *New J. Chem.* **2002**, *26*, 1529.
(26) Ramachandram, B.; Samanta, A. *Chem. Commun.* **1997**, 1037.
(27) Kim, H. N.; Lee, M. H.; Kim, H. J.; Kim, J. S.; Yoon, J. *Chem. Soc. Rev.* **2008**, *37*, 1453.
(28) Valeur, B. *Molecular Fluorescence: Principles and Applications*; Wiley-VCH Verlag GmbH: New York, 2001.
(29) Xiang, Y.; Tong, A.; Jin, P.; Ju, Y. *Org. Lett.* **2006**, *8*, 2863.
(30) Dujols, V.; Ford, F.; Czarnik, A. W. *J. Am. Chem. Soc.* **1997**, *119*, 7386.
(31) Kim, Y.-R.; Kim, H. J.; Kim, J. S.; Kim, H. *Adv. Mater.* **2008**, *20*, 4428.
(32) Kwon, J. Y.; Jang, Y. J.; Lee, Y. J.; Kim, K. M.; Seo, M. S.; Nam, W.; Yoon, J. *J. Am. Chem. Soc.* **2005**, *127*, 10107.
(33) Zhan, X. Q.; Qian, Z. H.; Zheng, H.; Su, B. Y.; Lan, Z.; Xu, J. G. *Chem. Commun.* **2008**, 1859.
(34) Huang, J.; Xu, Y.; Qian, X. *J. Org. Chem.* **2009**, *74*, 2167.
(35) Wu, J. S.; Hwang, I. C.; Kim, K. S.; Kim, J. S. *Org. Lett.* **2007**, *9*, 907.
(36) Zheng, H.; Qian, Z. H.; Xu, L.; Yuan, F. F.; Lan, L. D.; Xu, J. G. *Org. Lett.* **2006**, *8*, 859.
(37) Lee, M. L.; Wu, J. S.; Lee, J. W.; Jung, J. H.; Kim, J. S. *Org. Lett.* **2007**, *9*, 2501.
(38) Ko, S. K.; Yang, Y. K.; Tae, J.; Shin, I. *J. Am. Chem. Soc.* **2006**, *128*, 14150.
(39) yang, H.; Zhou, Z. G.; Huang, K. W.; Yu, M. X.; Li, F. Y.; Yi, T.; Huang, C. H. *Org. Lett.* **2007**, *9*, 4729.
(40) Huang, W.; Song, C.; He, C.; Lv, G.; Hu, X.; Zhu, X.; Duan, C. *Inorg. Chem.* **2009**, *48*, 5061.
(41) Chen, X.; Nam, S.-W.; Jou, M. J.; Kim, Y.; Kim, S.-J.; Park, S.; Yoon, J. *Org. Lett.* **2008**, *10*, 5235.
(42) Weerasinghe, A. J.; Shmiesing, C.; Sinn, E. *Tetrahedron Lett.* **2009**, *50*, 6407.
(43) Denk, W.; Strickler, J. H.; Webb, W. W. *Science* **1990**, *248*, 73.
(44) Dela Cruz, J. M.; Pastirk, I.; Comstock, M.; Lozovoy, V. V.; Dantus, M. *Proc. Natl. Acad. Sci. U.S.A.* **2004**, *101*, 16996.
(45) Thompson, C.; Keeley, D. L.; Pollock, K. M.; Dvornic, P. R.; Keinath, S. E.; Dantus, M.; Gunaratne, T. C.; LeCaptain, D. J. *Chem. Mater.* **2008**, *20*, 2829.
(46) Narayanan, A.; Varnavski, O. P.; Swager, T. M.; Goodson, T., III *J. Phys. Chem. C* **2008**, *112*, 881.
(47) Bhaskar, A.; Ramakrishna, G.; Twieg, R J.; Goodson, T., III *J. Phys. Chem. C* **2007**, *111*, 14607.
(48) Sumalekshmy, S.; Henary, M. M.; Siegel, N.; Lawson, P V.; Wu, Y.; Schmidt, K.; Brédas, J.-L.; Perry, J. W.; Fahrni, C. J. *J. Am. Chem. Soc.* **2007**, *129*, 11888.
(49) Zhang, X.; Ren, X.; Xu, Q.-H.; Loh, K. P.; Chen, Z.-K. *Org. Lett.* **2009**, *11*, 1257.
(50) Varaganti, S.; Gessesse, M.; Obare, S. O.; Ramakrishna, G. *Proc. SPIE* **2009**, *7413*, 741309741309−10.
(51) Makarov, N. S.; Dorbizhev, M.; Rebance, A. *Opt. Exp.* **2008**, *6*, 4029.
(52) Ramakrishna, G.; Goodson, T. III; Rogers-Haley, J. E.; Cooper, T. M.; McLean, D. G.; Urbas, A. *J. Phys. Chem. C* **2009**, *113*, 1060.
(53) Connors, K. A. *Binding Constants-The Measurement of Molecular Complex Stability*; John Wiley & Sons: New York, 1987.

JP1034568